

University of Groningen

A surface-bound molecule that undergoes optically biased Brownian rotation

Hutchison, James A.; Uji-i, Hiroshi; Deres, Ania; Vosch, Tom; Rocha, Susana; Müller, Sibylle; Bastian, Andreas A.; Enderlein, Jörg; Nourouzi, Hassan; Li, Chen

Published in:
Nature Nanotechnology

DOI:
[10.1038/nnano.2013.285](https://doi.org/10.1038/nnano.2013.285)

IMPORTANT NOTE: You are advised to consult the publisher's version (publisher's PDF) if you wish to cite from it. Please check the document version below.

Document Version
Publisher's PDF, also known as Version of record

Publication date:
2014

[Link to publication in University of Groningen/UMCG research database](#)

Citation for published version (APA):

Hutchison, J. A., Uji-i, H., Deres, A., Vosch, T., Rocha, S., Müller, S., Bastian, A. A., Enderlein, J., Nourouzi, H., Li, C., Herrmann, A., Müllen, K., Schryver, F. D., & Hofkens, J. (2014). A surface-bound molecule that undergoes optically biased Brownian rotation. *Nature Nanotechnology*, 9(2), 131-136. <https://doi.org/10.1038/nnano.2013.285>

Copyright

Other than for strictly personal use, it is not permitted to download or to forward/distribute the text or part of it without the consent of the author(s) and/or copyright holder(s), unless the work is under an open content license (like Creative Commons).

The publication may also be distributed here under the terms of Article 25fa of the Dutch Copyright Act, indicated by the "Taverne" license. More information can be found on the University of Groningen website: <https://www.rug.nl/library/open-access/self-archiving-pure/taverne-amendment>.

Take-down policy

If you believe that this document breaches copyright please contact us providing details, and we will remove access to the work immediately and investigate your claim.

Downloaded from the University of Groningen/UMCG research database (Pure): <http://www.rug.nl/research/portal>. For technical reasons the number of authors shown on this cover page is limited to 10 maximum.

A surface-bound molecule that undergoes optically biased Brownian rotation

James A. Hutchison, Hiroshi Uji-i, Ania Deres, Tom Vosch, Susana Rocha, Sibylle Müller, Andreas A. Bastian, Jörg Enderlein, Hassan Nourouzi, Chen Li, Andreas Herrmann, Klaus Müllen, Frans De Schryver, and Johan Hofkens.

Sections:

S1: Methods, materials, synthetic overviews and individual procedures: Perylene imides..	Page SI 02
S2: Methods, materials, synthetic overviews and individual procedures: Terrylene imides..	Page SI 17
S3: Materials and methods for optical and computational studies.....	Page SI 21
S4: Choosing appropriate image integration times for defocused fluorescence imaging.....	Page SI 22
Supplementary Figure S1: Defocused fluorescence images as a function of image integration time.	
S5: Analysis of rotational dynamics of 2	Page SI 23
Supplementary Figure S2: Frequency histograms of polar and azimuthal angles of the perylene imide subunit of the single molecules of 2 .	
S6: In-plane field distribution for wide-field q-TIRF excitation.....	Page SI 25
Supplementary Figure S3: Incident angle dependence of optical field intensities for q-TIRF excitation.	
S7: Bulk, solution phase photophysics of 1-3	Page SI 26
Supplementary Figure S4: Absorption and emission of 1 and 2 in ethanol.	
Supplementary Figure S5: Transient absorption spectroscopy of 2 in aerated methanol.	
Supplementary Figure S6: Absorption and emission spectra of 3 in ethanol.	
S8: Description of Supplementary Videos.....	Page SI 29
S9: References.....	Page SI 29

Section S1: Methods, materials, synthetic overviews and individual procedures:**Perylene imides****General methods for synthesis:**

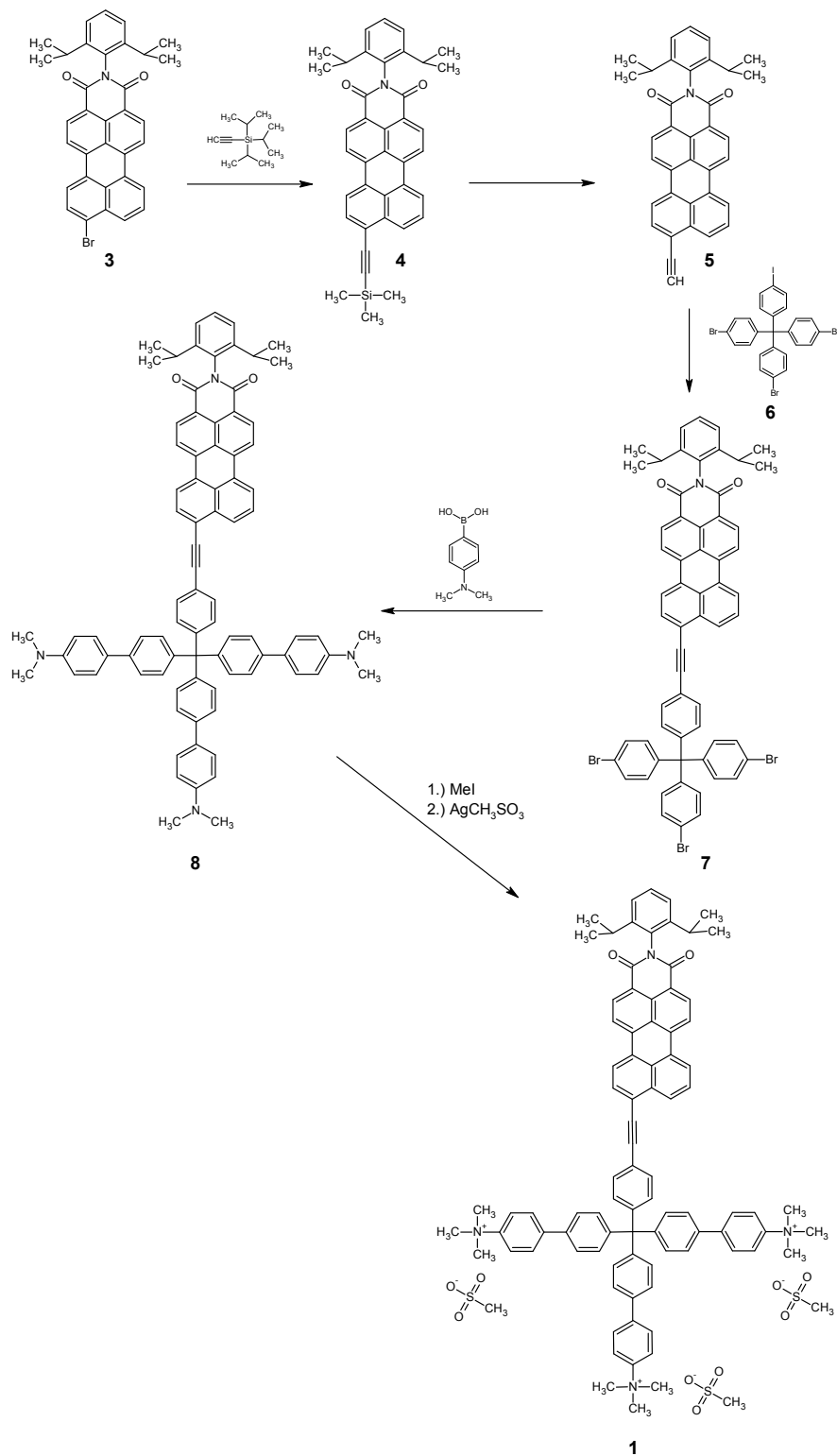
^1H -NMR- and ^{13}C -NMR-spectra were recorded on “Bruker Avance 250”, “Bruker AMC 300”, “Bruker DRX 500” and “Bruker AMX700”. Field desorption mass spectrometry was carried out on “ZAB 2-SE-FPD – instrument” (*VG instruments*). MALDI-TOF-mass spectra were recorded using “Bruker-Reflex-device” employing a LSI-N₂-laser. IR-spectroscopy was carried out on “FT-IR-spectrometer 320” (*Nicolet*) using Suprasil-quartz cuvette (1cm, *Hellma*). UV/Vis-spectra were recorded on “Lambda 15-spectrometer” (*Perkin Elmer*) using Suprasil-quartz cuvette (1cm, *Hellma*). Fluorescence spectroscopy was carried out on “SPEX USA Fluorolog 2 type F212” with a Xenon lamp XBO (450W, *Osram*) and the photomultiplier detectors “PMT R 508” and “PMT R 928” (*Hamatsu*) using Suprasil-quartz cuvette (1cm, *Hellma*). Elemental analysis was carried out on “Foss Heraeus Vario EL” at the Institute of Organic Chemistry at the Johannes Gutenberg-University (Mainz, Germany).

Materials for synthesis:

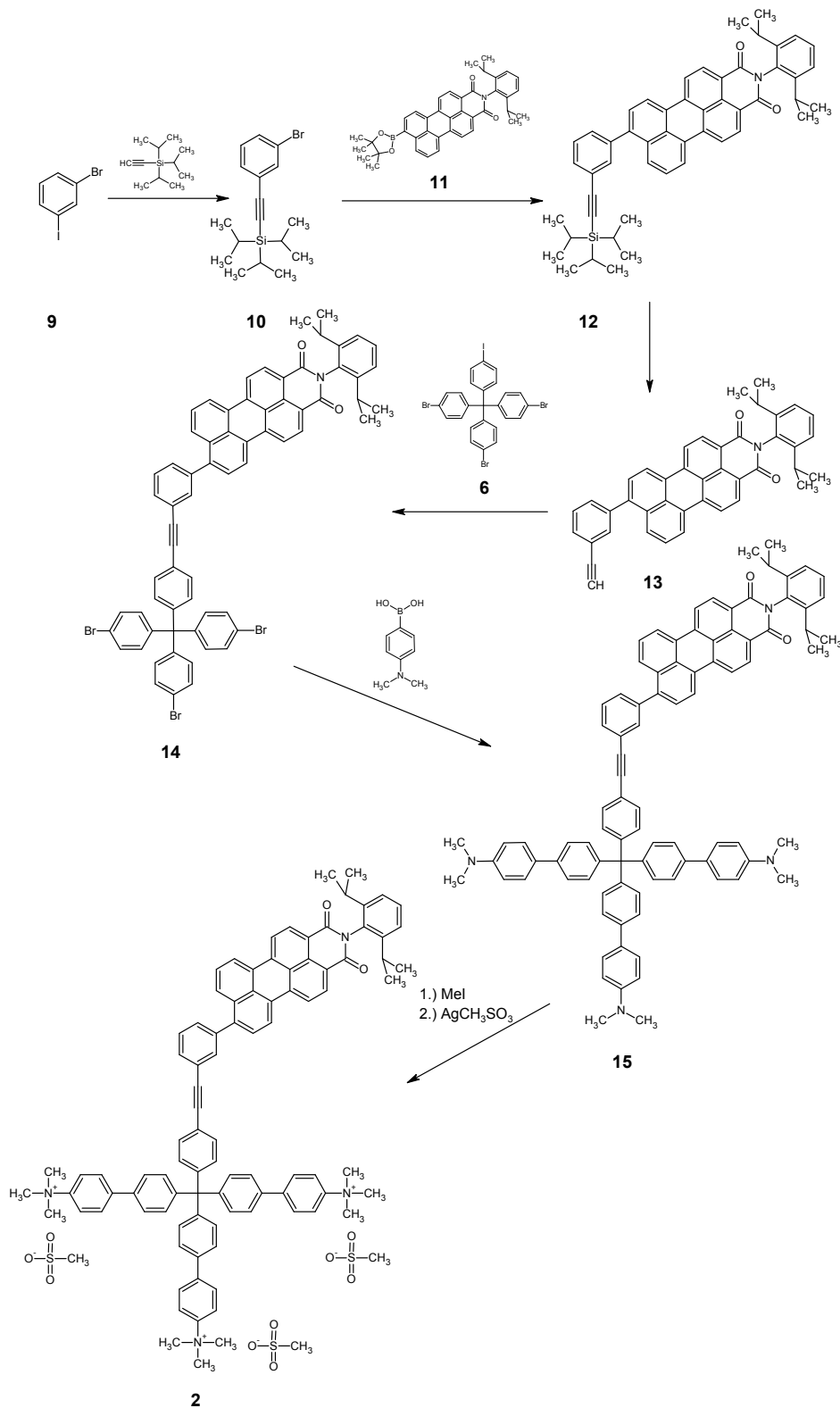
All chemicals and reagents were purchased from *ABCR*, *Acros*, *Aldrich*, *Fluka*, *Lancaster*, *Merck* and *Riedel-de-Haën* and were used without further purification unless otherwise noted. Utilized solvents were dried as described in the relevant literature. Deuterated solvents were purchased from *Deutero GmbH*. The applied perylene starting Materials were provided from the laboratories of *BASF AG* (Ludwigshafen, Germany). Silica-TLC plates with fluorescence indicator F_{254} were purchased from *Machery-Nagel*. For column chromatography silica gel was used with a particle size of 0.063-0.200 mm (*Merck*). Argon (*Linde*) was applied as inert gas.

Synthetic schemes of compounds 1, 2 and 6.

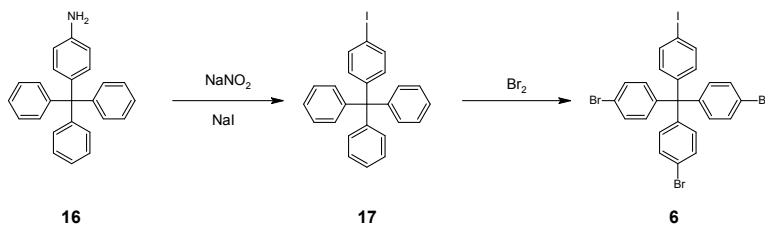
Synthetic scheme of compound 1.



Synthetic scheme of compound 2.

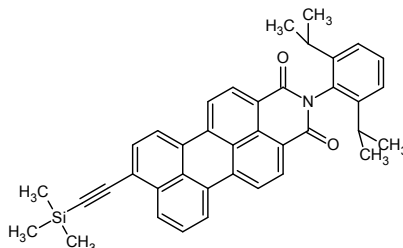


Synthetic scheme of compound 6.



Individual procedures:

***N*-(2',6'-Diisopropylphenyl)-9-trimethylsilylethynyl-3,4-perylene-dicarboxylic acid monoimide**
(4)



N-(2',6'-diisopropylphenyl)-9-bromo-3,4-perpylene-dicarboxylic acid monoimide (**3**) (1.5 g, 2.68 mmol), tetrakis-(triphenylphosphine)palladium(0) (62 mg, 0.054 mmol) and copper iodide (5 mg, 0.027 mmol) were dissolved in a 1:1 mixture of piperidine and THF (200 mL). The mixture was closed with a septum and stirred for 10 minutes at 70 °C. Then trimethylsilyl acetylene (0.79 g, 8.04 mmol) was added using a syringe and the reaction mixture was stirred at 80 °C. After 10 hours reaction time dichloromethane (200 mL) and a 1:1 mixture of conc. HCl and water (750 mL) were added. The organic layer was washed several times with water and dried using magnesium sulfate. After the solution was concentrated under vacuum the residue was purified by column chromatography using silica gel and a 2:1 mixture of petroleum ether and dichloromethane as eluent.

yield: 1.01 g (1.90 mmol) bright yellow solid (71 %).

¹H-NMR (300 MHz, C₂D₂Cl₄, 293 K) δ [ppm]: 8.50 (d, ³J = 8.02 Hz, 1H); 8.49 (d, ³J = 8.40 Hz, 1H); 8.30 (m, 4H); 8.20 (d, ³J = 8.01 Hz, 1H); 7.71 (d, ³J = 7.63 Hz, 1H); 7.61 (t, ³J = 8.01 Hz, 1H); 7.40 (dd, ³J = 7.62 Hz, ³J = 8.02 Hz, 1H); 7.25 (d, ³J = 7.63 Hz, 2H); 2.65 (sept, ³J = 6.87 Hz, 2H, CH(CH₃)₂); 1.09 (d, ³J = 6.87 Hz, 12 H, CH(CH₃)₂); 0.32 (s, 9 H, Si-CH₃).

¹³C-NMR (75 MHz, C₂D₂Cl₄, 293 K) δ [ppm]: 164.03 (C=O); 145.87; 137.45; 137.02; 134.53; 132.20; 132.09; 132.03; 131.46; 130.59; 129.67; 129.51; 128.06; 127.85; 126.93; 124.53; 124.24; 123.93; 123.29; 121.48; 121.32; 121.16; 120.86; 104.15 (C≡C); 102.65 (C≡C); 29.40 (CH(CH₃)₂); 24.35 (CH(CH₃)₂); 0.38 (Si-CH₃).

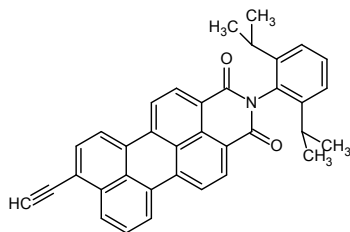
UV-Vis (chloroform): λ_{max} (ϵ) = 266 nm ($35600 \text{ M}^{-1} \text{ cm}^{-1}$); 499 nm ($42100 \text{ M}^{-1} \text{ cm}^{-1}$); 526 nm ($43500 \text{ M}^{-1} \text{ cm}^{-1}$).

IR (KBr): ν [cm^{-1}]: 3063; 2960; 2927; 2868; 2359; 2342; 2143; 1702; 1665; 1591; 1573; 1468; 1407; 1354; 1292; 1245; 1196; 1178; 1128; 862; 843; 825; 807; 762; 751; 738; 665; 627; 445.

FD-MS (8 kV): m/z = 577.6 (100 %) [M^+] (calc. for $\text{C}_{39}\text{H}_{35}\text{NO}_2\text{Si}$: 577.807).

Elemental analysis: calc.: 81.07 % C; 6.11 % H; 2.42 % N; found: 80.71 % C; 5.98 %; H 2.18 % N.

***N*-(2',6'-Diisopropylphenyl)-9-ethynyl-3,4-perylene-dicarboxylic acid monoimide (5)**



N-(2',6'-Diisopropylphenyl)-9-trimethylsilylethynyl-3,4-perylene-dicarboxylic acid monoimide (**4**) (2 g, 3.46 mmol) was dissolved in dry THF (150 mL). Then a solution of *n*-tetrabutylammonium fluoride (0.9 g, 3.46 mmol) in THF (20 mL) was added under inert atmosphere. After stirring for 15 minutes at room temperature the reaction mixture was diluted with dichloromethane (250 mL) and washed with water. The combined organic layers were washed with a 1:1 mixture of conc. HCl and water and once again with water. The combined organic solutions were dried using magnesium sulfate, concentrated under reduced pressure and the residue was purified by column chromatography using silica gel and dichloromethane as eluent.

yield: 0.79 g (2.24 mmol) red solid (74 %).

$^1\text{H-NMR}$ (300 MHz, CD_2Cl_2 , 293 K) δ [ppm]: 8.55 (d, 3J = 8.01 Hz, 1H); 8.54 (d, 3J = 8.01 Hz, 1H); 8.40 (m, 4H); 8.30 (d, 3J = 8.01 Hz, 1H); 7.78 (d, 3J = 7.63 Hz, 1H); 7.67 (t, 3J = 8.01 Hz, 1H), 7.39 (dd, 3J = 7.63 Hz, 3J = 8.01 Hz, 1H); 7.24 (d, 3J = 7.63 Hz, 2H); 3.67 (s, 1H, $\text{C}\equiv\text{C-H}$); 2.64 (sept, 3J = 6.87 Hz, 2H, $\text{CH}(\text{CH}_3)_2$); 1.09 (d, 3J = 6.87 Hz, 13 H, $\text{CH}(\text{CH}_3)_2$).

$^{13}\text{C-NMR}$ (75 MHz, CD_2Cl_2 , 293 K) δ [ppm]: 164.02 (C=O); 145.88; 137.44; 136.98; 134.75; 132.49; 132.31; 132.18; 131.41; 130.62; 130.21; 129.69; 129.49; 129.37; 128.30; 127.94; 127.03; 124.65; 124.25; 123.25; 122.79; 121.70; 121.45; 121.35; 121.05; 85.70 ($\text{C}\equiv\text{C-H}$); 81.71 ($\text{C}\equiv\text{C-H}$); 29.39 ($\text{CH}(\text{CH}_3)_2$); 24.36 ($\text{CH}(\text{CH}_3)_2$).

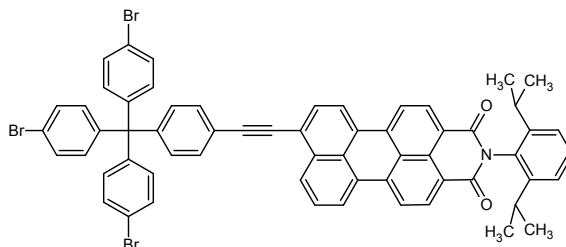
UV-Vis (chloroform): λ_{max} (ϵ) = 244 nm ($37500 \text{ M}^{-1} \text{ cm}^{-1}$); 265 nm ($34200 \text{ M}^{-1} \text{ cm}^{-1}$); 491 nm ($38900 \text{ M}^{-1} \text{ cm}^{-1}$); 518 nm ($40500 \text{ M}^{-1} \text{ cm}^{-1}$).

IR (KBr): ν [cm^{-1}]: 2960; 2927; 2868; 2359; 2342; 2143; 1702; 1665; 1591; 1573; 1468; 1407; 1356; 1292; 1245; 1196; 1178; 1128; 861; 842; 825; 807; 762; 751; 738; 455.

FD-MS (8 kV): m/z = 505.6 (100 %) [M^+] (calc. for $\text{C}_{36}\text{H}_{27}\text{NO}_2$: 504.6).

Elemental analysis: calc.: 85.69 % C; 5.19 % H; 2.78 % N; found: 85.42 % C; 5.51 % H; 2.68 % N.

***N*-(2',6'-Diisopropylphenyl)-9-((tri-(4''-bromophenyl)-methyl)-phenylethynyl)-3,4-perylene-dicarboxylic acid monoimide (7)**



Iodo-(4-tri-(4'-bromophenyl)-methyl)-benzene (**6**) (288 g, 0.422 mmol), bis-(triphenylphosphine)palladium(II) dichloride (67 mg, 0.095 mmol), triphenylphosphine (25 mg, 0.095 mmol) and copper iodide (18 mg, 0.095 mmol) were dissolved in a mixture of triethylamine (30 mL) and dry THF (15 mL). After addition of *N*-(2',6'-diisopropylphenyl)-9-ethynyl-3,4-perylene-dicarboxylic acid monoimide (**5**) (320 mg, 0.633 mmol) the reaction mixture was flashed with argon and stirred for 16 hour at room temperature in darkness. To the reaction a 1:3 mixture of conc. HCl and water (200 mL) was added and the mixture was extracted with dichloromethane several times. The combined organic layers were dried using magnesium sulfate and were concentrated under vacuum. The residue was purified by column chromatography using dichloromethane as eluent.

yield: 306 mg (0.288 mmol) red solid (68.4 %); **R_f-value:** 0.85 (dichloromethane)

¹H-NMR (500 MHz, CD₂Cl₂, 306 K) δ [ppm]: 8.60 (d, ³J = 7.9 Hz, 1H); 8.59 (d, ³J = 7.9 Hz, 1H); 8.41 – 8.36 (m, 3H); 8.33 (d, ³J = 8.2 Hz, 1H); 8.25 (d, ³J = 8.2 Hz, 1H); 7.74 (d, ³J = 7.9 Hz, 1H); 7.64 – 7.63 (m, 3H); 7.52 (t, ³J = 7.9 Hz, 3H); 7.45 (d, ³J = 8.8 Hz, 6H); 7.36 (d, ³J = 7.9 Hz, 2H); 7.27 (d, ³J = 8.5 Hz, 2H); 7.12 (d, ³J = 8.8 Hz, 6H); 2.79 (sept., ³J = 6.6 Hz, 2H); 1.17 (d, ³J = 7.9 Hz, 12H). **¹³C-NMR (125 MHz, CD₂Cl₂, 306 K, spin echo experiment)** δ [ppm]: 164.37 (C=O); 164.35 (C=O); 146.84 (q); 146.50 (q); 145.06 (q); 139.51 (q); 137.47 (q); 137.05 (q); 134.35 (q); 133.87 (q); 132.93 (t); 132.19 (t); 132.07 (t); 131.97 (q); 131.72 (t); 131.62 (t); 131.46 (t); 131.33 (t); 130.78 (q); 129.71 (t); 129.65 (q); 129.32 (t); 127.89 (t); 126.95 (q); 124.64 (t); 124.41 (t); 123.94 (q); 123.50 (t); 121.44 (q); 121.13 (t); 121.02 (q); 120.94 (t); 119.33 (q); 118.11 (q); 97.50 (C≡C); 88.08 (C≡C); 64.50 (CPh₄); 29.52 (CH(CH₃)₂); 24.12 (CH(CH₃)₂).

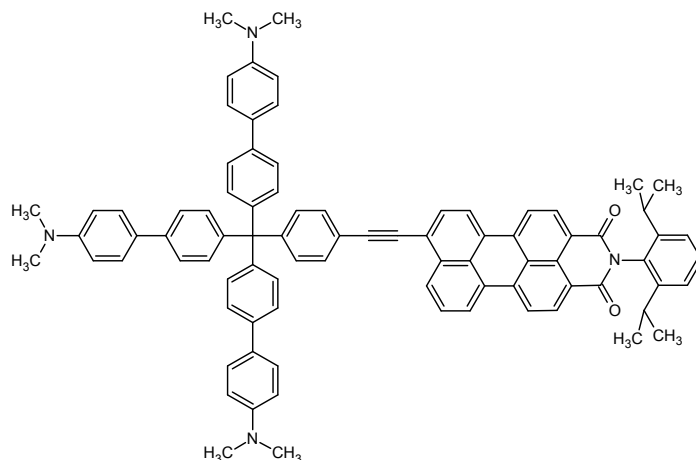
UV-Vis (chloroform) λ_{max} (ε) = 508 nm (45000 M⁻¹ cm⁻¹); 534 nm (48000 M⁻¹ cm⁻¹)

IR (KBr): ν [cm⁻¹]: 2960, 2927, 2868, 2366, 1701, 1664, 1572, 1485, 1358, 1244, 1006, 810, 752

FD-MS (8 kV): m/z = 1059.4 (100 %) [M⁺] (calc. for C₆₁H₄₂Br₃NO₂: 1060.73).

Elemental analysis: calc.: 69.07 % C; 3.99 % H; 1.32 % N; found: 68.99 % C; 4.01 % H; 1.34 % N.

***N*-(2',6'-diisopropylphenyl)-9-((tri-(4''(4'''-*N,N*-dimethylaminophenyl)-phenyl)-methyl)-phenylethynyl)-3,4-perylene-dicarboxylic acid monoimide (8)**



N-(2',6'-diisopropylphenyl)-9-((tri-(4''-bromophenyl)-methyl)-phenylethynyl)-3,4-perylene-dicarboxylic acid monoimide (**7**) (150 mg, 0.141 mmol), 4-(dimethylamino)phenyl boronic acid (233 mg, 1.414 mmol), and tetrakis-(triphenylphosphine)-palladium(0) (50mg, 0.042 mmol) were dissolved in toluene (25 mL), ethanol (1 mL) and 2M aqueous solution of potassium carbonate (10 mL). The reaction mixture was flashed with argon and stirred for 16 hour at 75 °C under inert atmosphere. The reaction was cooled down to room temperature and the organic layer was separated. The aqueous solution was extracted with toluene several times and the organic layers were combined, dried using magnesium sulfate and concentrated. The crude mixture was purified by column chromatography using 2% ethanol solution in dichloromethane as eluent.

yield: 117 mg (0.099 mmol) red solid (70.2 %); **R_f-value:** 0.63 (dichloromethane + 2 % ethanol).

¹H-NMR (500 MHz, CD₂Cl₂, 306 K) δ [ppm]: 8.64 (dd, ³J = 8.2 Hz, 4J = 2.2 Hz, 2H); 8.54 (t, ³J = 7.6 Hz, 2H); 8.50 (d, ³J = 8.2 Hz, 1H); 8.47 (d, ³J = 8.6 Hz, 1H); 8.43 (d, ³J = 8.2 Hz, 1H), 7.87 (d, ³J = 7.9 Hz, 1H); 7.75 (t, ³J = 7.9 Hz, 1H); 7.65 (d, ³J = 8.5 Hz, 2H); 7.54 – 7.48 (m, 11H); 7.43 – 7.35 (m, 12H); 6.79 (d, ³J = 8.8 Hz, 6H); 2.98 (s, 18H); 2.77 (sept., ³J = 6.6 Hz, 2H); 1.15 (d, ³J = 6.9 Hz, 12H).

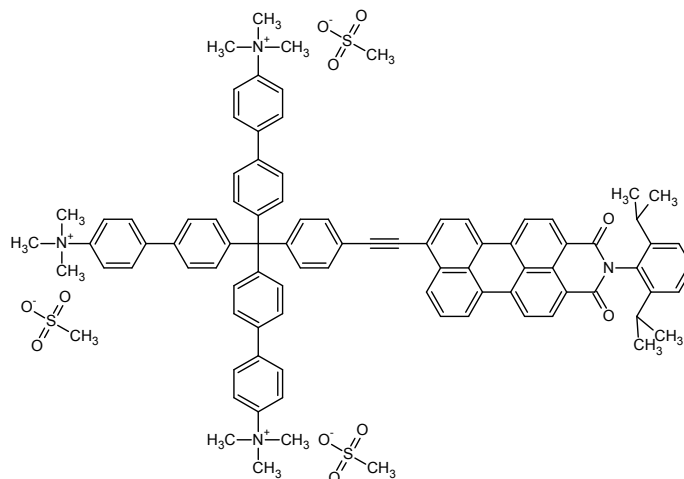
¹³C-NMR (125 MHz, CD₂Cl₂, 306 K) δ [ppm]: 164.40 (C=O); 150.58; 149.01; 146.56; 144.73; 139.09; 137.75; 137.39; 134.59; 132.26; 132.01; 131.69; 131.63; 131.42; 130.94; 129.86; 129.68; 129.36; 128.55; 128.46; 128.26; 128.12; 127.97; 127.75; 127.22; 126.96; 125.63; 124.83; 124.39; 121.63; 121.55; 121.23; 121.05; 120.63; 113.37; 113.02; 98.13 (C≡C); 87.73 (C≡C); 64.76 (CPh₄); 40.67 (N-CH₃); 29.50 (CH(CH₃)₂); 24.01 (CH(CH₃)₂).

UV-Vis (chloroform): λ_{max} (ε) = 513 nm (43000 M⁻¹ cm⁻¹); 536 nm (45000 M⁻¹ cm⁻¹).

IR (KBr): ν [cm⁻¹]: 2962, 2927, 2870, 2810, 2366, 1701, 1655, 1610, 1593, 1498, 1444, 1358, 1292, 1244, 1198, 1059, 1016, 947, 808, 752, 669.

FD-MS (8 kV): m/z = 1181.2 (100 %) [M⁺]; 590.9 (19 %) [M²⁺] (calc. for C₈₅H₇₂N₄O₂: 1181.56).

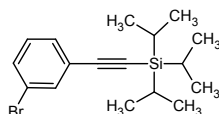
***N*-(2',6'-Diisopropylphenyl)-9-((tri-(4''(4'''-*N,N*'-trimethylammomiumphenyl)-phenyl)-methyl)-phenylethynyl)-3,4-perylene-dicarboxylic acid monoimide methylsulfonate (1)**



N-(2',6'-Diisopropylphenyl)-9-((tri-(4''(4'''-*N,N*'-dimethylaminophenyl)-phenyl)-methyl)-phenylethynyl)-3,4-perylene-dicarboxylic acid monoimide (**8**) (50 mg, 0.042 mmol) was dissolved in chloroform (15 mL) at 75 °C and iodomethane (1 mL) was added. After the reaction mixture was stirred overnight the solution was concentrated under reduced pressure and the residue was dissolved in methanol. The resulting solution was again treated with iodomethane (1 mL) and stirred at 80 °C. After a reaction time of 10 h the solvent was evaporated and the residue was dried under reduced pressure. The resulting red solid was dissolved in methanol (20 mL) and silver methanesulfonate (14.8 mg, 0.073 mmol) was added. After the reaction mixture was stirred overnight the precipitate was filtrated. The filtrate was concentrated under reduced pressure and the resulting residue was purified by dialysis in water (membrane permeability <500 g/mol).

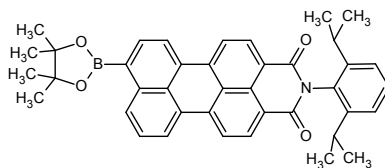
yield: 20 mg (0.013 mmol) red solid (31 %).

3-Bromo-triisopropylsilyl-ethynyl-benzene (10)



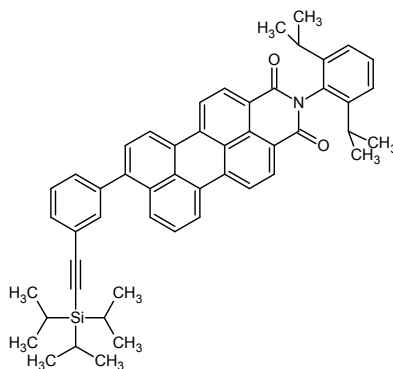
Compound **10** was synthesized as described in the literature: B. Felber, F. Diederich, *Helv. Chim. Act.* **2005**, 88, 120-153

***N*-(2',6'-Diisopropylphenyl)-9-(4'',4'',5'',5''-tetramethyl-1'',3'',2''-dioxaborolan-2''-yl)-3,4-perylene-dicarboxylic acid monoimide (11)**



Compound **11** was synthesized as described in the literature: T. Weil, E. Reuther, C. Beer, K. Müllen, *Chem. Eur. J.* **2004**, 10, 1398-1414.

***N*-(2',6'-Diisopropylphenyl)-9-(3''-(triisopropylsilyl)ethynyl)-phenyl)-3,4-perylene-dicarboxylic acid monoimide (12)**



3-Bromo-triisopropylsilyl ethynyl-benzene (**10**) (1.1g, 3.292 mmol), *N*-(2',6'-diisopropylphenyl)-9-(4'',4'',5'',5''-tetramethyl-1'',3'',2''-dioxaborolan-2''-yl)-3,4-perylene-dicarboxylic acid monoimide (**11**) (500 mg, 0.823 mmol), and tetrakis(triphenylphosphine)-palladium(0) (76 mg, 0.066 mmol) were dissolved in mixture of toluene (50 mL), ethanol (5 mL) and 2M aqueous solution of potassium carbonate (15 mL). The reaction mixture was flushed with argon and stirred for four days at 75 °C under inert atmosphere. The reaction was cooled down to room temperature and the organic layer was separated. The aqueous solution was extracted with toluene several times. The combined organic layers were dried using magnesium sulfate, concentrated and the resulting residue was purified by column chromatography using silica gel and dichloromethane as eluent.

yield: 447 mg (0.606 mmol) red solid (73.6 %); **R_f-value:** 0.57 (dichloromethane).

¹H-NMR (500 MHz, C₂D₂Cl₄, 306 K) δ [ppm]: 8.56 (d, ³J = 7.9 Hz, 2H); 8.46 – 8.42 (m, 4H); 7.90 (d, ³J = 8.4 Hz, 1H); 7.60 – 7.54 (m, 4H); 7.44 – 7.43 (m, 2H); 7.39 (t, 3J = 7.9 Hz, 1H); 7.25 (d, ³J = 7.8 Hz, 2H); 2.65 (sept., ³J = 6.9 Hz, 2H); 1.08 (d, ³J = 6.9 Hz, 12H); 1.07 (s, 21H). **¹³C-NMR (125 MHz, C₂D₂Cl₄, 306 K, spin echo experiment)** δ [ppm]: 164.12 (C=O); 145.85 (q); 142.66 (q); 140.08 (q); 138.00 (q); 137.77 (q); 133.53 (t); 132.73 (q); 132.32 (t); 132.04 (t); 131.47 (q); 130.73 (q); 130.33 (t); 129.61(q); 129.55 (t); 129.44 (t); 128.99(q); 128.83 (t); 128.68 (t); 128.50 (q); 127.65 (t); 127.14 (q),

124.45 (t); 124.30 (q); 124.26 (t); 123.94 (t); 121.18 (q); 121.13 (q); 120.81(t); 120.61 (t); 106.73 (C≡C); 91.96 (C≡C); 29.36 (CH(CH₃)₂); 24.39 (CH(CH₃)₂); 19.06 (Si-CH(CH₃)₂); 11.60 (Si-CH(CH₃)₂).

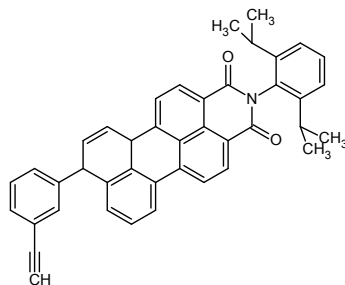
UV-Vis (chloroform): λ_{max} (ε) = 494 nm (41000 M⁻¹ cm⁻¹); 517 nm (40000 M⁻¹ cm⁻¹). **fluorescence (chloroform, λ_{exc}. 480 nm):** λ_{max} = 563 nm.

IR (KBr): n [cm⁻¹]: 2962, 2866, 2364, 2160, 1703, 1662, 1593, 1577, 1460, 1358, 1244, 812

FD-MS (8 kV): m/z = 738.9 (100 %) [M⁺] (calc. for C₅₁H₅₁NO₂Si: 738.07).

Elemental analysis: calc.: 83.00 % C; 6.97 % H; 1.90 % N; found: 82.93 % C; 7.01 % H; 1.91 % N

***N*-(2',6'-Diisopropylphenyl)-9-(3''-ethynylphenyl)-3,4-perylene-dicarboxylic acid monoimide (13)**



N-(2',6'-Diisopropylphenyl)-9-(3''-(triisopropylsilyl)ethynyl)-phenyl)-3,4-perylene-dicarboxylic acid monoimide (**12**) (300 mg, 0.474 mmol) was dissolved in dry THF (15 mL). Then a solution of *n*-tetrabutylammonium fluoride (224 mg, 0.711 mmol) in THF (2 mL) was added under inert atmosphere. After stirring for seven minutes at room temperature the reaction mixture was quenched with water (60 mL) and the crude mixture was extracted with dichloromethane. The combined organic layers were dried using magnesium sulfate, concentrated under reduced pressure and the residue was purified by column chromatography using silica gel and dichloromethane as eluent.

yield: 256 mg (0.440 mmol) red solid (92.8 %); **R_f-value:** 0.56 (dichloromethane).

¹H-NMR (500 MHz, CD₂Cl₂, 306 K) δ [ppm]: 8.56 (d, ³J = 8.1 Hz, 2H); 8.46 – 8.43 (m, 4H); 7.89 (d, ³J = 8.5 Hz, 1H); 7.63 (s, 1H); 7.58 – 7.53 (m, 3H); 7.50 – 7.45 (m, 2H), 7.39 (t, ³J = 8.1 Hz, 1H); 7.25 (d, ³J = 8.1 Hz, 2H); 3.14 (s, 1H); 2.66 (sept., ³J = 6.8 Hz, 2H); 1.09 (d, ³J = 6.8 Hz, 12H). **¹³C-NMR (125 MHz, CD₂Cl₂, 306 K, spin echo experiment)** δ [ppm]: 164.11 (C=O); 145.88 (q); 142.42 (q); 140.22 (q); 137.97 (q); 137.74 (q); 133.81 (t); 132.69 (q); 132.30 (t); 132.01 (t); 131.49 (q); 130.83 (t); 130.73 (q); 129.64 (q); 129.44 (t); 129.44 (t); 129.08(q); 129.03 (t); 128.66 (t); 128.54 (q), 127.68 (t); 127.15 (q), 124.44 (t); 124.25 (t); 123.90 (t); 122.69 (q); 121.23 (q); 121.20 (q); 120.84 (t); 120.66 (t); 83.74 (C≡C-H); 78.56 (C≡C-H); 29.37 (CH(CH₃)₂); 24.37 (CH(CH₃)₂).

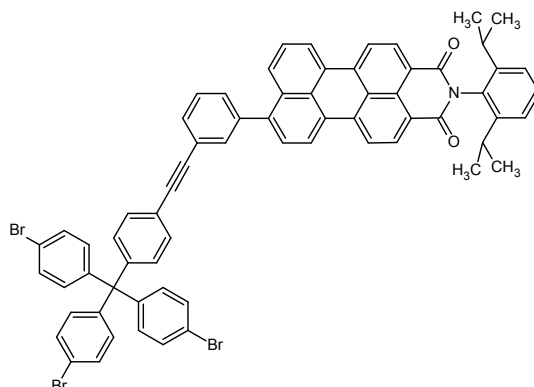
UV-Vis (chloroform): λ_{max} (ε) = 494 nm (36000 M⁻¹ cm⁻¹); 519 nm (35000 M⁻¹ cm⁻¹).

IR (KBr): n [cm⁻¹]: 2962, 2933, 2868, 2119, 1701, 1660, 1593, 1572, 1468, 1360, 1294, 1244, 810, 754.

FD-MS (8 kV): m/z = 582.2 (100 %) [M⁺] (calc. for C₄₂H₃₁NO₂: 581.72).

Elemental analysis: calc.: 86.72 % C; 5.37 % H; 2.41 % N; found: 86.78 % C; 5.36 % H; 2.35 % N.

***N*-(2',6'-Diisopropylphenyl)-9-(3''-(tri-(4'''-bromophenyl)-methyl)-ethynylphenyl)-3,4-perylene-dicarboxylic acid monoimide (14)**



Iodo-(4-tri-(4'-bromophenyl)-methyl)-benzene (**6**) (156 g, 0.229 mmol), bis-(triphenylphosphine)palladium(II) dichloride (36 mg, 0.052 mmol), triphenylphosphine (14 mg, 0.052 mmol) and copper iodide (10 mg, 0.052 mmol) were dissolved in a mixture of triethylamine (30 mL) and dry THF (15 mL). After addition of *N*-(2',6'-diisopropylphenyl)-9-(3''-ethynyl)-3,4-perylene-dicarboxylic acid monoimide (**13**) (200 mg, 0.344 mmol) the reaction mixture was flashed with argon and stirred for 16 hour at room temperature in darkness. To the reaction a 1:3 mixture of conc. HCl and water (200 mL) was added and the mixture was extracted with dichloromethane several times. The combined organic layers were dried using magnesium sulfate and concentrated under vacuum. The residue was purified by column chromatography using silica gel and dichloromethane as eluent.

yield: 230 mg (0.202 mmol) red solid (88.4 %); **R_f-value:** 0.75 (dichloromethane).

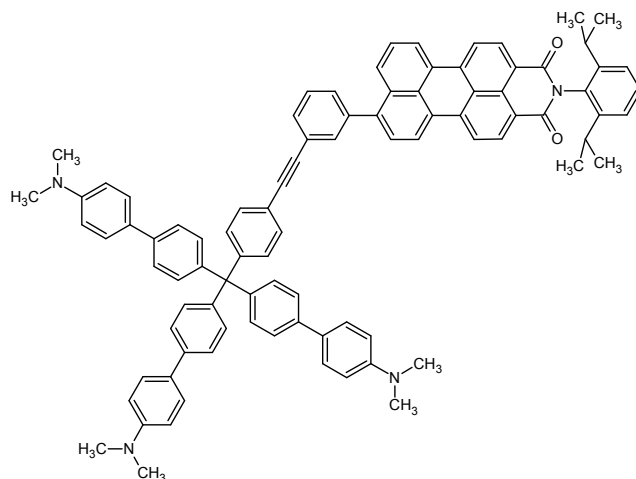
¹H-NMR (700 MHz, C₂D₂Cl₄, 393 K) δ [ppm]: 8.61 (d, ³J = 8.0 Hz, 1H); 8.60 (d, ³J = 8.0 Hz, 1H); 8.49 – 8.45 (m, 4H); 7.93 (d, ³J = 8.6 Hz, 1H), 7.69 (s, 1H); 7.61 – 7.58 (m, 2H); 7.50 – 7.49 (m, 1H); 7.44 (d, ³J = 8.4 Hz, 2H); 7.40 – 7.38 (m, 6H); 7.27 (d, ³J = 7.8 Hz, 2H); 7.20 (t, ³J = 7.7 Hz, 1H); 7.12 (d, ³J = 8.6 Hz, 4H); 7.01 (d, ³J = 8.7 Hz, 6H); 2.74 (sept., ³J = 6.9 Hz, 2H); 1.15 (d, ³J = 6.9 Hz, 12H). **¹³C-NMR (175 MHz, C₂D₂Cl₄, 293 K, spin echo experiment)** δ [ppm]: 164.12 (C=O); 146.06 (q); 145.86 (q); 144.84 (q); 142.59 (q); 140.24 (q); 138.28 (q); 138.00 (q); 137.77 (q); 136.84 (t); 133.32 (t); 132.70 (q); 132.64 (t); 132.32 (t); 131.65 (t); 131.42 (t); 130.91 (t); 130.74 (q); 130.42 (t); 129.63 (q); 129.44 (t); 129.11 (t); 129.03 (q); 128.69 (t); 128.60 (t); 128.54 (q); 127.68 (t); 127.15 (q); 123.67 (q); 125.70 (t); 124.47 (t); 124.26 (t); 123.96 (t); 121.35 (q); 121.19 (q); 121.15 (q); 120.91 (q); 120.84 (t); 120.65 (t); 90.03 (C≡C); 89.88 (C≡C); 64.22 (CC₄); 29.30(CH(CH₃)₂); 24.41 (CH(CH₃)₂).

UV-Vis (chloroform): λ_{max} (ε) = 496 nm (46000 M⁻¹ cm⁻¹); 520 nm (45000 M⁻¹ cm⁻¹).

IR (KBr): ν [cm⁻¹]: 2962, 2929, 2870, 1701, 1662, 1591, 1574, 1485, 1360, 1246, 1009, 812, 756.

FD-MS (8 kV): m/z = 1137.9 (100 %) [M⁺] (calc. for C₆₇H₄₆Br₃NO₂: 1136.83).

***N*-(2',6'-Diisopropylphenyl)-9-(3''-(tri-(4'''-*N,N*-dimethylaminophenyl)-phenyl)-methyl)-ethynylphenyl)-phenyl-3,4-perylene-dicarboxylic acid monoimide (**15**)**



N-(2',6'-Diisopropylphenyl)-9-(3''-(tri-(4'''-bromophenyl)-methyl)-ethynylphenyl)-phenyl-3,4-perylene-dicarboxylic acid monoimide (**14**) (150 mg, 0.132 mmol), 4-(dimethylamino)phenyl boronic acid (218 mg, 1.320 mmol), and tetrakis-(triphenylphosphine)-palladium(0) (50 mg, 0.040 mmol) were dissolved in toluene (25 mL), ethanol (2 mL) and 2M aqueous solution of potassium carbonate (10 mL). The reaction mixture was flashed with argon and stirred for three days at 75 °C under inert atmosphere. The reaction was cooled down to room temperature and the organic layer was separated. The aqueous solution was extracted with toluene several times and the organic layers were combined, dried using magnesium sulfate and concentrated. The crude mixture was purified by column chromatography using silica gel and 2% ethanol solution in dichloromethane as eluent.

yield: 140 mg (0.111 mmol) red solid (84.3 %); **R_f-value:** 0.67 (dichloromethane + 2 % ethanol).

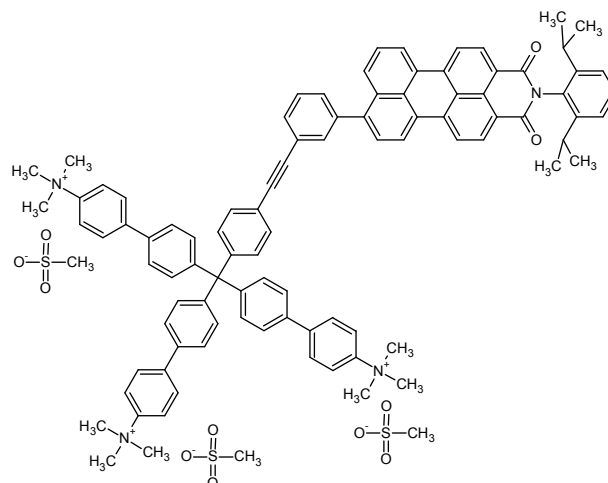
¹H-NMR (700 MHz, C₂D₂Cl₄, 293 K) δ [ppm]: 8.56 (d, ³J = 7.6 Hz, 2H); 8.47 – 8.43 (m, 4H); 7.95 (d, ³J = 7.7 Hz, 1H), 7.68 (s, 1H); 7.61 (d, ³J = 6.9 Hz, 1H); 7.58 – 7.57 (m, 2H); 7.46 (d, ³J = 7.7 Hz, 6H); 7.47 – 7.42 (m, 9H); 7.38 (t, ³J = 7.7 Hz, 2H); 7.27 (d, ³J = 8.5 Hz, 2H); 7.26 – 7.23 (m, 8H); 6.71 (d, ³J = 7.7 Hz, 6H); 2.91 (s, 18H); 2.66 (sept., ³J = 6.8 Hz, 2H); 1.09 (d, ³J = 6.8 Hz, 12H). **¹³C-NMR (175 MHz, C₂D₂Cl₄, 293 K, spin echo experiment)** δ [ppm]: 164.12 (C=O); 150.14 (q); 148.23 (q); 145.89 (q); 144.49 (q); 142.70 (q); 140.21 (q); 138.42 (q); 138.03 (q); 137.81 (q); 133.32 (t); 132.73 (q); 132.30 (t); 131.75 (q); 131.62 (t); 131.49 (t); 131.21 (t); 130.74 (q); 130.20 (t); 129.61 (q); 129.58 (t); 129.42 (t); 129.28 (t); 129.06 (t); 129.00 (q); 128.69 (t); 128.55 (q); 128.25 (q); 127.69 (t); 127.16 (q); 125.33 (t); 124.45 (t); 124.24 (t); 123.97 (t); 121.19 (q); 121.15 (q); 120.80 (t); 120.62 (t); 120.46 (q); 90.48 (C≡C); 89.51 (C≡C); 64.43 (C₄); 40.83 (NCH₃); 29.33 (CH(CH₃)₂); 24.37 (CH(CH₃)₂).

UV-Vis (chloroform): λ_{max} (ε) = 497 nm (42000 M⁻¹ cm⁻¹); 520 nm (41000 M⁻¹ cm⁻¹).

IR (KBr): ν [cm⁻¹]: 3028, 2962, 2870, 2802, 2362, 1699, 1660, 1610, 1576, 1498, 1442, 1358, 1196, 945, 808.

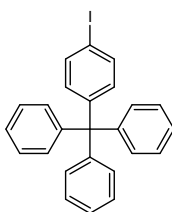
FD-MS (8 kV): m/z = 1137.9 (100 %) [M⁺] (calc. for C₉₁H₇₆N₄O₂: 1136.83).

***N*-(2',6'-Diisopropylphenyl)-9-(3''-(tri-(4'''(4'''-*N,N*'-trimethylammoniumphenyl)-phenyl)-methyl)-ethynylphenyl)-phenyl-3,4-perylene-dicarboxylic acid methylsulfonate (2)**



N-(2',6'-diisopropylphenyl)-9-(3''-(tri-(4'''(4'''-*N,N*'-dimethylaminophenyl)-phenyl)-methyl)-ethynylphenyl)-phenyl-3,4-perylene-dicarboxylic acid monoimide (**15**) (25 mg, 0.020 mmol) was dissolved in chloroform (15 mL) at 75 °C and iodomethane (1 mL) was added. After the reaction mixture was stirred overnight, the solution was concentrated under reduced pressure and the residue was dissolved in methanol. The resulting solution was again treated with iodomethane (1 mL) and stirred at 80 °C. After 10 hour reaction time the solvent was evaporated and the residue was dried under reduced pressure. The resulting red solid was dissolved in methanol (10 mL) and silver methanesulfonate (7.4 mg, 0.036 mmol) was added. After the reaction mixture was stirred overnight the precipitate was filtrated. The filtrate was concentrated under reduced pressure and the resulting residue was purified by dialysis in water (membrane permeability <500 g/mol).

yield: 26.3 mg (0.017 mmol) red solid (82.7 %).

Iodo-4-(triphenylmethyl)-benzene (17)

4-(Triphenylmethyl)-aniline (**16**) (10 g, 29.811 mmol) was suspended carefully in a 1:3 mixture of conc. sulfuric acid and water not exceeding a temperature of 50 °C. The suspension was cooled to 5 °C and a solution of sodium nitrite (2.01 g, 29.811 mmol) in water (12 mL) was added drop wise not exceeding a temperature of 8 °C. Then the yellow colored suspension was added drop wise (25 min) into a solution of sodium iodide (4.47 g, 29.821 mmol) in water (14 mL). The brown-violet mixture was stirred for one hour at room temperature and then additionally for 30 minutes at 100 °C. After the reaction mixture was cooled down to room temperature 1M aqueous solution of sodium sulfite (approx. 200 mL) was added until the yellow color disappeared. After filtration of the suspension the filter cake was washed with water and dried. The yellow-brown solid was purified by column chromatography using silica gel and dichloromethane as eluent.

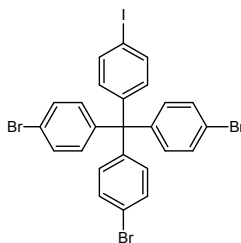
yield: 10.1 g (22.656 mmol) yellow solid (76.2 %); **R_f-value:** 0.98 (dichloromethane).

¹H-NMR (250 MHz, CD₂Cl₂, 293 K) δ [ppm]: 7.58 (d, ³J = 8.9 Hz, 2H); 7.22 (m, 15H); 7.01 (d, ³J = 8.9 Hz, 2H). **¹³C-NMR (62.5 MHz, d8-THF, 293 K)** δ [ppm]: 147.35; 146.79; 137.02; 133.55; 131.31; 128.05; 126.47; 91.86 (Cl); 65.22 (CPh₄).

IR (KBr): ν [cm⁻¹]: 3060, 1595, 1491, 1441, 1003, 818, 764, 750, 702, 633.

FD-MS (8 kV): m/z = 446.1 (100 %) [M⁺] (calc. for C₂₅H₁₉I: 446.33).

Elemental analysis: calc.: 67.28 % C; 4.29 % H; found: 67.27 % C; 4.27 % H.

Iodo-4-(tri-(4'-bromophenyl)-methyl)-benzene (6)

Iodo-4-(triphenylmethyl)-benzene (**17**) (500 mg, 1.130 mmol) was stirred in bromine (2 mL) for 45 minutes at room temperature. The mixture was cooled to 0 °C and ice cold ethanol (25 mL) was added. After dichloromethane (30 mL) and an aqueous solution of sodium thiosulfate (30 mL) were

added the organic layer was separated and the aqueous solution was extracted with dichloromethane several times. The combined organic layers were dried using magnesium sulfate and concentrated under vacuum. The yellow solid was taken up in dichloromethane and purified by column chromatography using first petroleum ether and then dichloromethane as eluent.

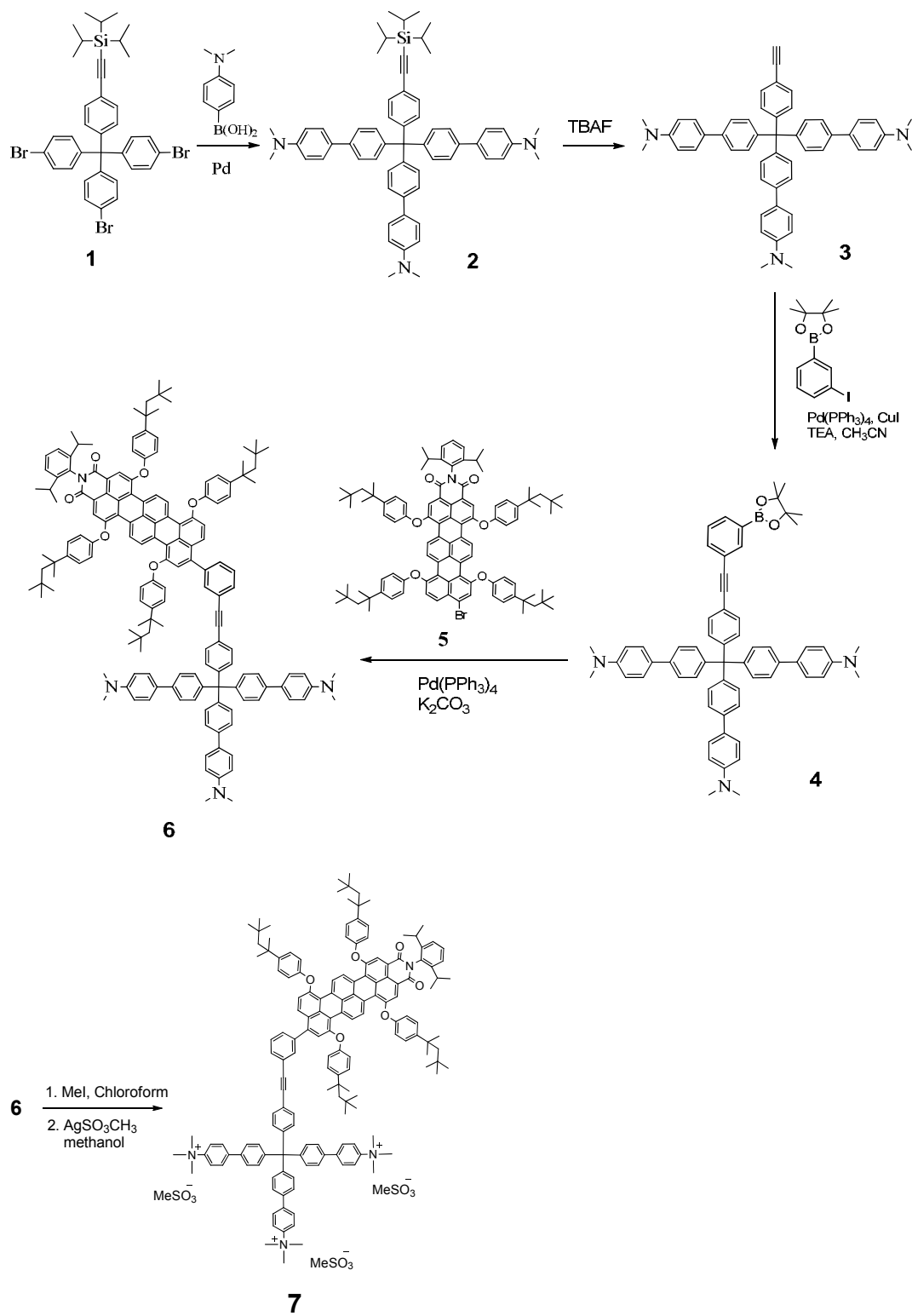
yield: 560 mg (0.820 mmol) bright yellow solid (96.3 %); **R_f-value:** 0.63 (petroleum ether)

¹H-NMR (500 MHz, CD₂Cl₂, 306 K) δ [ppm]: 7.61 (d, ³J = 8.9 Hz, 2H); 7.41 (d, ³J = 8.6 Hz, 6H); 7.04 (d, ³J = 8.9 Hz, 6H); 6.91 (d, ³J = 8.9 Hz, 2H). **¹³C-NMR (62.5 MHz, d8-THF, 293 K)** δ [ppm]: 145.70; 144.94; 137.43; 133.07; 132.83; 131.39; 120.97 (CBr); 92.58 (Cl); 64.17 (CPh₄).

IR (KBr): ν [cm⁻¹]: 3064, 1570, 1479, 1396, 1078, 1009, 808.

FD-MS (8 kV): m/z = 686.0 (100 %) [M⁺] (calc. for C₂₅H₁₆Br₃I: 683.02).

Elemental analysis: calc.: 43.96 % C; 2.36 % H; found: 43.96 % C; 2.40 % H.

Section S2: Methods, materials, synthetic overviews and individual procedures:**Terrylene imide**

General methods: ^1H and ^{13}C NMR spectra were recorded on Bruker AMX250, Bruker AC300, AMX500 NMR and AMX700 NMR spectrometers using the residual proton or the carbon signal of the deuterated solvent as an internal standard. Chemical shifts are reported in parts per million. FD mass spectra were performed with a VG-Instrument ZAB 2-SE-FDP. High Resolution Mass spectra (HRMS) were recorded with a Finnigan MAT and VG Instruments ZAB 2-SE-FPD. UV/Vis absorption spectra were recorded on a Perkin Elmer Lambda 900 spectrophotometer. The elemental analyses were carried out by the Microanalytical Laboratory of Johannes Gutenberg University.

Materials: Solvents and Pd-catalysts were purchased from Aldrich. Column chromatography was performed with dichloromethane, methanol, pentane or toluene on silica gel (Geduran Si60, Merck). N-(2,6-diisopropylphenyl)-1,6,9,14-tetrakis(p-tert-octylphenoxy)-terrylene-3,4-dicarboximide was supplied from BASF-SE (Ludwigshafen). All reported yields are isolated yields.

4-{4-[bis({4-[4-(dimethylamino)phenyl]phenyl})(4-ethynylphenyl)methyl]phenyl}-N,N-dimethylaniline (3):

TBAF (1M solution in THF, 0.35 mmol) was added to a solution of tri-*isopropylsilyl*-(tri-(4'-(4''-N',N'-dimethylaminophenyl)-phenyl)-methyl)-phenylacetylene (200 mg, 0.23 mmol) in 10 mL THF at 0°C. After 4 h of stirring at this temperature, the reaction was quenched by adding 10 ml of water and was extracted with dichloromethane. The organic phases were combined, dried over magnesium sulfate and concentrated *in vacuo*. The resulting residue was purified by flash column chromatography (SiO_2 ; DCM) to afford **3** (150 mg, 92%) as a beige solid.

^1H -NMR (300 MHz, CD_2Cl_2 , 293 K):

δ [ppm]: 7.52 – 7.38 (m, 16H) 7.36-7.28 (m, 8H), 6.77 (d, J = 8.85 Hz, 4H), 3.10 (s, 1H), 2.96 (s, 18H).

^{13}C -NMR (75 MHz, CD_2Cl_2 , 293 K):

δ [ppm]: 150.25, 148.40, 144.41, 138.73, 131.42, 131.35, 131.13, 128.16, 127.44, 125.23, 119.58, 112.77, 83.56, 77.06, 64.31, 40.37.

High Resolution MALDI-TOF ($\text{C}_{51}\text{H}_{47}\text{N}_3$) calculated 701.3770, Found 701.3778.
Elemental analysis (%) calcd. for $\text{C}_{51}\text{H}_{47}\text{N}_3$ (701.94): C, 87.26; H, 6.75; N, 5.99;
found: C 87.38, H 6.68, N 5.83.

4-{4-[bis({4-[4-(dimethylamino)phenyl]phenyl})(4-{2-[3-(tetramethyl-1,3,2-dioxaborolan-2-yl)phenyl]ethynyl}phenyl)methyl]phenyl}-N,N-dimethylaniline (4):

CuI (0.072 g, 0.38 mmol) and Pd(PPh₃)₄ (0.22 g, 0.19 mmol) were added to a solution of **3** (100 mg, 0.142 mmol), 3-iodobenzeneboronic acid pinacol ester (47 mg, 0.142 mmol) and triethylamine (58 μ L, 0.426 mmol) in dry CH₃CN (30 mL) under argon. The mixture was degassed and stirred for 4 h at 70°C under argon. The reaction mixture was then allowed to cool to room temperature and solvent was evaporated to dryness under reduced pressure. The solid was solubilized in dichloromethane and filtered through a pad of silica. Purification of the resulting residue by GPC afforded **4** (98 mg, 76%) as a beige solid.

¹H-NMR (300 MHz, CD₂Cl₂, 293 K):

δ [ppm]: 7.94 – 7.97 (m, 1H), 7.73 (dt, J = 7.6, 1.3 Hz, 1H), 7.62 (dt, J = 7.6, 1.3 Hz, 1H), 7.56–7.53 (m, 5H), 7.51–7.48 (m, 7H), 7.47–7.45 (m, 1H), 7.41–7.32 (m, 10H), 6.80 (d, J = 8.91 Hz, 6H), 2.98 (s, 18H), 1.34 (s, 12H).

¹³C-NMR (75 MHz, CD₂Cl₂, 293 K):

δ [ppm]: 150.73, 148.29, 145.01, 139.19, 138.47, 134.82, 134.57, 131.88, 131.69, 131.37, 128.69, 128.37, 127.94, 125.72, 123.43, 121.31, 113.26, 89.90, 89.80, 84.62, 64.82, 40.87, 25.27.

High Resolution MALDI-TOF (C₆₃H₆₂BN₃O₂) calculated 903.4935, Found 903.4941. Elemental analysis (%) calcd. for C₆₃H₆₂BN₃O₂ (904.00): C, 83.70; H, 6.91; N, 4.65; found: C 83.82, H 6.81, N 4.56.

N-(2,6-Diisopropylphenyl)-11-bromo-1,6,9,14-tetrakis(*p*-*tert*-octylphenoxy)-terrylene-3,4-dicarboximide (5**):**

A solution of N-(2,6-diisopropylphenyl)-1,6,9,14-tetrakis(*p*-*tert*-octylphenoxy)-terrylene-3,4-dicarboximide (480 mg, 0.32 mmol), N-bromosuccinimide (NBS) (170 mg, 0.96 mmol) in dry THF was fluxed for 6 h under an argon atmosphere. After removal of solvent, further purification by column chromatography by using toluene as eluent to yield 95 %.

¹H-NMR Spectrum (300 MHz, CD₂Cl₂, 300 K):

δ [ppm]: 9.24 (t, 2H), 9.03 (d, J = 9 Hz, 1H), 8.95 (d, J = 9 Hz, 1H), 8.09 (s, 1H), 8.05 (s, 1H), 7.87 (d, J = 9 Hz, 1H), 7.39–7.27(m, 10H), 7.22 (d, J = 8 Hz, 2H), 7.03–6.89 (m, 9H), 2.61 (m, 2H), 1.65 (m, 8H), 1.29 (m, 24H), 1.01 (m, 12H), 0.67 (m, 36H);

¹³C-NMR (75 MHz, CD₂Cl₂, 300 K):

δ [ppm]: 163.6, 163.6, 155.8, 154.4, 154.0, 153.8, 153.8, 153.7, 153.6, 146.7, 146.6, 146.4, 132.5, 131.7, 131.6, 130.6, 130.5, 129.7, 129.6, 129.3, 128.3, 128.3, 128.1, 127.3, 127.3, 126.8, 126.7, 125.5, 124.3, 123.8, 123.8, 123.6, 123.5, 121.0, 120.0, 119.1, 118.9, 118.8, 108.9, 66.9, 66.6, 57.4, 50.7, 38.6, 34.2, 34.1, 32.5, 31.9, 31.8, 31.7, 31.6, 31.6, 30.0, 29.3, 28.6, 24.0.

IR Spectrum (KBr): ν_{\max} = 2952, 1701, 1664, 1595, 1500, 1315, 1277, 1211, 1171, 1095, 1055, 1014, 901, 876, 831, 735 cm⁻¹.

UV/Vis (CH₂Cl₂): λ_{\max} (ϵ /M⁻¹cm⁻¹) : 644 (108616).

MS (FD): m/z 1501.5 (100%) [M⁺] (Calc. 1501.90).

Elemental Analysis (C₁₀₀H₁₁₀BrNO₆): Calculated: (%) C 79.97, H 7.38, N 0.93, Found: (%) C 75.91, H 7.40, N 0.81.

7-[2,6-bis(propan-2-yl)phenyl]-11,18,24,33- tetrakis[4-(2,4,4-trimethylpentan-2-yl)phenoxy]-20- [3-(2-{4-[tris({4-[4-(dimethylamino)phenyl]phenyl)methyl]phenyl}ethynyl)phenyl]-7-azanonacyclo[14.12.2.2^{2,5}.1^{17,21}.0^{3,12}.0^{4,9}.0^{13,29}.0^{26,30}.0^{25,31}]tritriaconta-1(28),2,4,9,11,13,15,17,19,21(31),22,24,26,29,32- pentadecaene-6,8-dione (6):

Potassium carbonate (1M, 0.026 mmol) was added to a solution of **5** (8 mg, 0.005 mmol), boronic ester **4** (9 mg, 0.010 mmol) and Pd(PPh₃)₄ (1.5 mg, 0.001 mmol) in 5 mL toluene and 0.2 mL ethanol. The mixture was degassed and stirred at 80°C overnight under argon. The reaction mixture was then allowed to cool to room temperature and solvent was evaporated to dryness under reduced pressure. The solid was solublized in dichloromethane and filtered through pad of silica. The crude product was purified by GPC to afford compound **6**, as a blue solid in 77% yield (9 mg).

¹H-NMR (500 MHz, CD₂Cl₂, 293 K):

δ [ppm]: 9.41 (dd, J = 9.0, 2.9 Hz, 2H), 9.17 (dd, J = 9.0, 1.0 Hz, 2H), 8.20 (s, 1H), 8.17 (s, 1H), 7.76 (d, J = 9.2 Hz, 1H), 7.59-7.28 (m, 37H), 7.13-7.01 (m, 10H), 6.78 (d, J = 8.9 Hz, 6H), 2.97 (s, 18H), 2.78-2.61 (m, 2H), 1.73-1.71 (m, 8H), 1.38-1.35 (m, 24H), 1.08 (d, J = 6.8 Hz, 12H), 0.72-0.66 (m, 36H).

¹³C-NMR (125 MHz, CD₂Cl₂, 293 K):

δ [ppm]: 163.89, 155.73, 155.22, 154.21, 154.16, 154.11, 150.68, 148.45, 146.88, 146.85, 146.65, 146.60, 146.53, 144.90, 141.72, 140.33, 139.16, 133.29, 132.87, 132.04, 131.82, 131.65, 131.48, 131.38, 130.38, 130.36, 130.04, 129.79, 129.69, 129.15, 128.59, 128.54, 128.52, 128.45, 128.34, 127.89, 126.85, 126.82, 125.67, 125.55, 124.53, 124.22, 124.13, 123.89, 121.33, 121.10, 120.95, 120.39, 119.99, 119.16, 119.07, 118.99, 113.19, 90.40, 89.42, 64.77, 57.61, 57.45, 40.84, 38.81, 38.77, 32.78, 32.10, 32.04, 31.93, 31.88, 31.84, 29.55, 24.26.

High Resolution MALDI-TOF (C₁₅₇H₁₆₀N₄O₆) calculated 2197.2338, Found 2197.2346.

4-[4-({4-[2-(3-{7-[2,6-bis(propan-2-yl)phenyl]-6,8- dioxo-11,18,24,33-tetrakis[4-(2,4,4- trimethylpentan-2-yl)phenoxy]-7-azanonacyclo[14.12.2.2^{2,5}.1^{17,21}.0^{3,12}.0^{4,9}.0^{13,29}.0^{26,30}.0^{25,31}]tritriaconta-1(28),2,4,9,11,13,15,17,19,21(31),22,24,26,29,32- pentadecaen-20-

yl}phenyl)ethynyl]phenyl}bis({4-[4-(trimethylazaniumyl)phenyl]phenyl})methyl}phenyl]- N,N,N-trimethylanilinium; tris(methanesulfonate) (7):

To a solution of **6** (9 mg, 0.005 mmol) in 5 mL chloroform, iodomethane (1 mL) was added. The resulting mixture was stirred overnight at 75 °C. The reaction mixture was then allowed to cool to room temperature and solvent was evaporated to dryness under reduced pressure. To the residue, methanol (5 mL) and iodomethane (1 mL) were added and was stirred overnight at 80 °C. After cooling to room temperature, solvent was evaporated to dryness under reduced pressure. The residue was dissolved in 5 mL methanol and silver methanesulfonate (5 mg, 0.025 mmol) was added. After stirring overnight at room temperature, the resulting precipitate was filtered and dried in high vacuum. For purification, the solid was subjected to a dialysis in water (membrane permeability $g < 500 \text{ mol}^{-1}$). Pure product was obtained as a blue solid in 77% yield (8 mg).

High Resolution MALDI-TOF ($\text{C}_{163}\text{H}_{178}\text{N}_4\text{O}_{15}\text{S}_3$) calculated 2527.2451, Found 2527.2458.

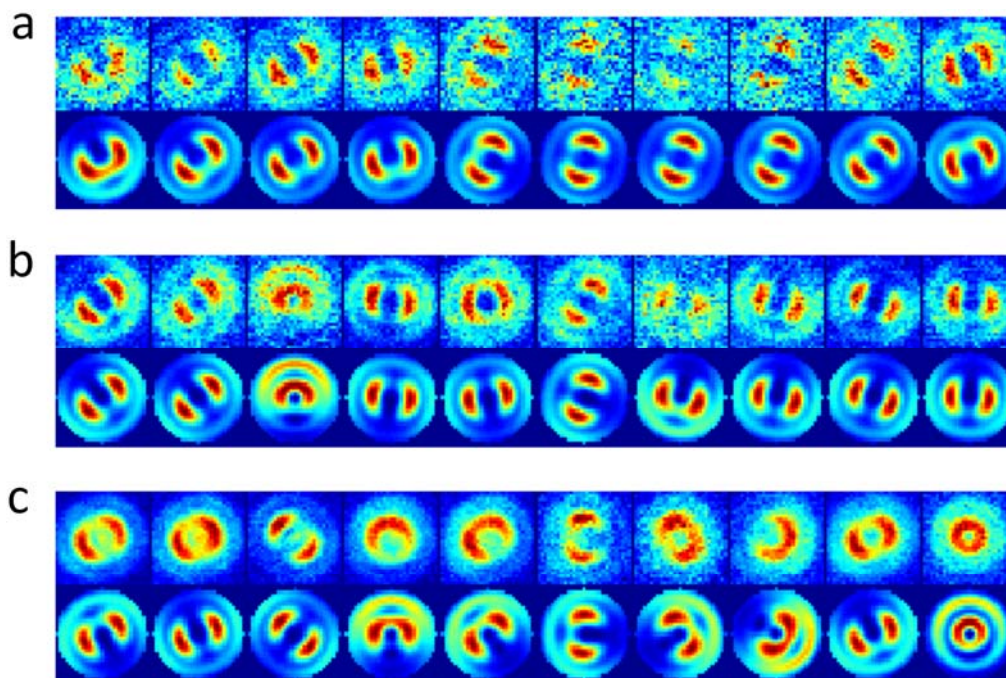
Section S3: Materials and methods for optical and computational studies

Borosilicate glass substrates were pre-cleaned by sonication in acetone, aqueous NaOH, and water, followed by U.V.-ozone treatment. Poly(n-butyl methacrylate) (MW = 10,200 g/mol, $T_g = 296 \text{ K}$) and styrene oligomer (MW = 360 g/mol, $T_g = 277 \text{ K}$) were purchased from Polymer Source, Inc. and used without further purification. Polymer over-layers were spin cast at ca. 3000 rpm from chloroform or toluene solutions (1% by weight polymer). Polymer layers were ca. 100 nm thick as measured by atomic force microscopy. The defocused wide-field fluorescence imaging was performed using an inverted optical microscope (IX71, Olympus) equipped with a 1.3-N.A. 100x oil immersion objective (Plan Fluorite, Olympus) and a CCD camera (cascade 512B, Princeton Instruments INC, iXon DV887 EMCCD, Andor Technology, or ImagEM, Hamamatsu). Diode-pumped solid-state lasers emitting continuous wave 532 nm light (for excitation of **1** and **2**) or 640 nm light (for excitation of **3**) were used as the excitation source. The excitation light was circularly polarized by using $\lambda/2$ plate and $\lambda/4$ before being focused at the back focal plane of the objective to achieve wide-field excitation. Fluorescence was collected by the same objective and passed through a dichroic mirror and a long pass filter to remove scattered excitation light. The image was further magnified 3.3 times with an additional lens (the resulting field of view is $24.6 \times 24.6 \mu\text{m}$). The excitation field contains only a limited contribution of radial or z-polarized light polarizations when focused at the centre of the back focal plane of the objective. The direction of light propagation is perpendicular to the substrate plane, and therefore the excitation of molecules with transition dipole moment oriented along the z-axis (perpendicular to the substrate plane) is disfavored.

To overcome this problem a quasi total internal reflection fluorescence excitation mode (q-TIRF) was employed, in which the excitation light was focused at the side of the objective such that it approached the substrate at high angle, generating evanescent fields polarized in the z-direction. Note that using an objective with NA of 1.3, only a part of the illumination can be reflected at a polymer/air interface and perfect TIRF illumination cannot be achieved. Defocused fluorescence images were analysed with a home-built MatLab routine according to theoretical models^{1,2}. A jacket around the objective and microscope stage allowed the temperature of the sample to be controlled with a thermostat water bath. Bulk fluorescence decays were measured using the time-correlated single photon counting technique. Transient absorption spectroscopy was undertaken using the amplified output of a titanium:sapphire laser (800 nm, 150 fs pulses of 1 mJ energy) coupled to an optical parametric oscillator. Energy minimisation was carried out using semi-empirical PM6 methods in Spartan 10 software (V. 1.1.0, Wavefunction Inc. California U.S.A.). Trialkylammonium groups were substituted by methyl groups to simplify the calculation. Transition dipole moment directions were calculated using Arguslab software (V. 4.0.1, Planaria Software LLC).

Section S4: Choosing appropriate integration times for defocused fluorescence imaging

The appropriate integration time for imaging in defocused wide-field fluorescence microscopy is long enough to have an image with adequate signal-to-noise for accurate orientation fitting, and short enough that no dynamic information is lost. In Fig. S1 below are examples of the same single molecule's orientation with time (discussed in the main text and featured in Fig. 3c), with image integration times 0.030 sec (Fig. S1a), 0.153 sec (Fig. S1b), and 1.53 sec (Fig. S1c). The images in Fig. S1b are obviously easier to fit than Fig. S1a, but have more likelihood of blurring the images of two orientations (possibly occurring in frame 5 of Fig. S1b). Rotational autocorrelation analysis yields exponential decays and rotation correlation times of 0.31 sec, 0.43 sec and 0.48 sec for image integration times of 0.03 sec, 0.09 sec, and 0.153 sec respectively. For much longer integration times (1.53 sec, Fig. S1c) the blurring is very obvious and the images are no longer able to be adequately fit. In summary, one should choose an integration time that is <30% of the rotational correlation time of the molecule to ensure reasonably accurate analysis. In this work we used integration times ~15% or less of the rotational correlation time of the molecule.



Supplementary Figure S1| Defocused fluorescence images as a function of image integration time. Defocused wide-field fluorescence images of a single molecule of **2** over time with image integration times of **a**, 0.03 sec **b**, 0.153 sec **c**, 1.53 sec. The upper panels are the raw image data, while the lower panels are the best-fit simulated patterns for extraction of orientation data.

Section S5: Analysis of rotational dynamics of 2

The autocorrelation functions ($C(t)$) of many observables for single molecule dynamics in glassy media are well fit by the Kohlrausch-Williams-Watts (KWW) or stretched exponential function³⁻⁶:

$$C(t) = \exp(-t / \tau_{\text{KWW}})^{\beta} \quad (\text{Eq. 1})$$

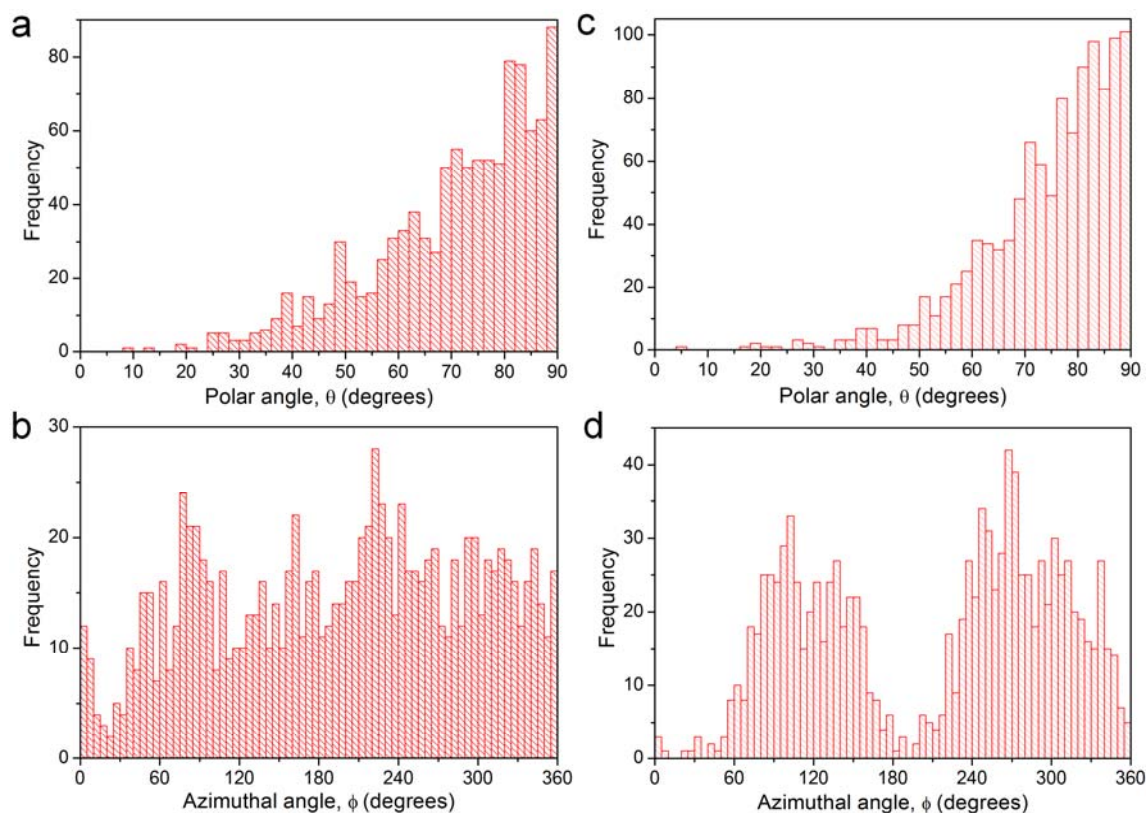
Where the relaxation time for the process (here the rotational correlation time, τ_c) is related to the measured decay time of the rotational autocorrelation function (τ_{KWW}) by:

$$\tau_c = (\tau_{\text{KWW}} / \beta) \Gamma(1 / \beta) \quad (\text{Eq. 2})$$

Γ is a gamma function and the stretch factor β is in the range $0 \leq \beta \leq 1$. Departure of β from 1 measures the degree of heterogeneity in the timescales of rotational diffusion experienced by the molecule over its survival time, imposed by heterogeneous relaxation of the matrix. Autocorrelation functions of the 3D angular displacement of the subset of molecules of the perylene imide rotor **2** typified in Fig. 3c of the main text yield a mean β value of 0.93 and a

mean τ_c of 0.25 seconds using this analysis (frequency histograms of the collected azimuthal and polar angles of the perylene imide subunit of the molecule featured in Fig. 3c of the main text are shown in Fig. S2a and b). Thus this subset of molecules of **2** display quasi-1-dimensional, random, thermally-driven rotational diffusion of their rylene subunit.

Autocorrelation functions of the 3D angular displacement of the subset of molecules of the perylene imide rotor **2** typified in Fig. 3d of the main text yield a mean β value of 0.69 and a mean τ_c of 0.99 seconds using this analysis (frequency histograms of the collected azimuthal and polar angles of the perylene imide subunit of the molecule featured in Fig. 3d of the main text are shown in Fig. S2c and d). This subset of molecules of **2** display more heterogeneity in the rotational diffusion environment of their rylene subunit, the rotation rate is slower, and the molecules display an unusual azimuthal orientational bias.

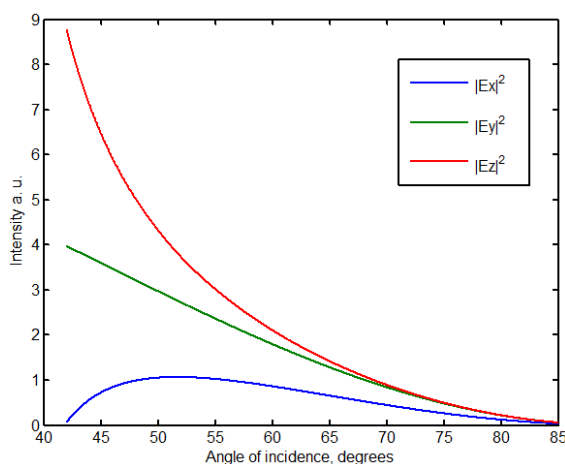


Supplementary Figure S2| Frequency histograms of polar and azimuthal angles of the perylene imide subunit of the single molecules of **2 featured in Fig. 3 of the main article.** Molecules under PnBMA at 315 K, image integration time 30 ms, **a**, Frequency histogram of the polar angle of the single molecule of **2** featured in Fig. 3c of the main article, bin width 2°. **b**, The azimuthal angles of the single molecule of **2** featured in Fig. 3c of the main article, bin width 5°. **c**, Frequency histogram of the polar angle of the single molecule of **2** featured in Fig. 3d of the main article, bin width 2°. **d**, The azimuthal angles of the single molecule of **2** featured in Fig. 3d of the main article, bin width 5°.

Section S6: In-plane field distribution for wide-field q-TIRF excitation

To generate wide-field excitation in these studies, a circularly polarized input laser beam was focused on the back focal plane of the microscope objective. The result was a collimated excitation beam $\sim 40\ \mu\text{m}$ diameter at the sample. If the excitation beam is aligned along the optical axis of the microscope (focused at the centre of the back focal plane of the objective) the excitation will pass through the sample at right angles, and the field amplitude will be equal in (and restricted to) all in-sample plane directions.

To generate quasi total internal reflection fluorescence (q-TIRF) excitation, the excitation beam is focused near the edge of the back focal plane of the objective so that it approaches the sample at a high angle. Here we will consider the case of the excitation beam approaching the surface along the in-plane x -direction. In this case, the p -polarized component of the excitation light generates an elliptically polarized evanescent field with components along the x - and z -directions (the z -direction is normal to the sample plane). Meanwhile the s -polarized component of the excitation light generates an evanescent field with identical penetration depth but purely polarized along the y -direction in-plane. The result is that in-plane evanescent field distribution is greater in the y -direction than it is in the x -direction, in which the evanescent field propagates (Fig. S3)⁷.

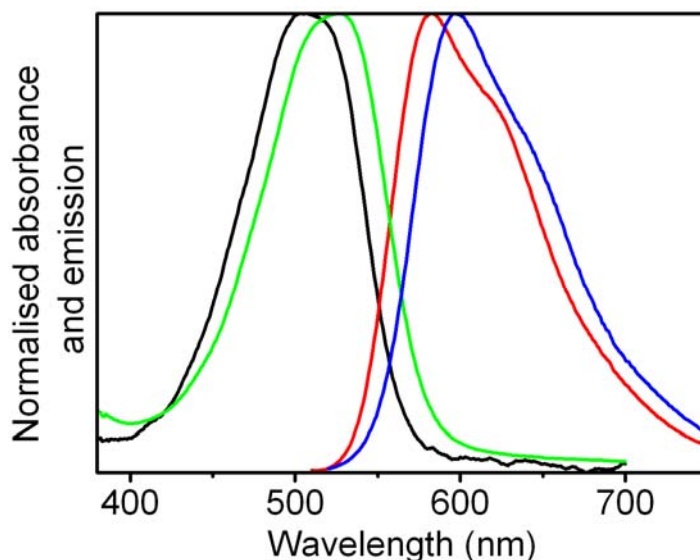


Supplementary Figure S3| Incident angle dependence of optical field intensities for q-TIRF excitation. For excitation light approaching an air/glass interface (refractive index of air(glass) = 1.0(1.5)) along the in-plane x -direction (z -direction is normal to the interface). The amplitudes ($|E|$) of the incident field p - and s -polarized components were set to be 1 and 1. Maximum incident angle using a NA = 1.3 objective is 60.07° and the ratio $|E_y|^2 / |E_x|^2$ at this incident angle is 2.0886.

Section S7: Bulk, solution photophysics of 1-3

The absorption and emission spectra of **1** are shown in Fig. S4, showing a 15-20 nm red-shift of the spectra in comparison with **2**, but with similar broadened features and >300 meV Stokes shift. The fluorescence quantum yields of **1** and **2** in ethanol are 0.51 and 0.82. While the fluorescence decay of **2** is mono-exponential ($\tau = 4.0$ ns, measured by the single photon counting technique), fluorescence from **1** decays with bi-exponential kinetics ($\tau_1 = 3.17$ ns (87%), $\tau_2 = 0.28$ ns (13%)).

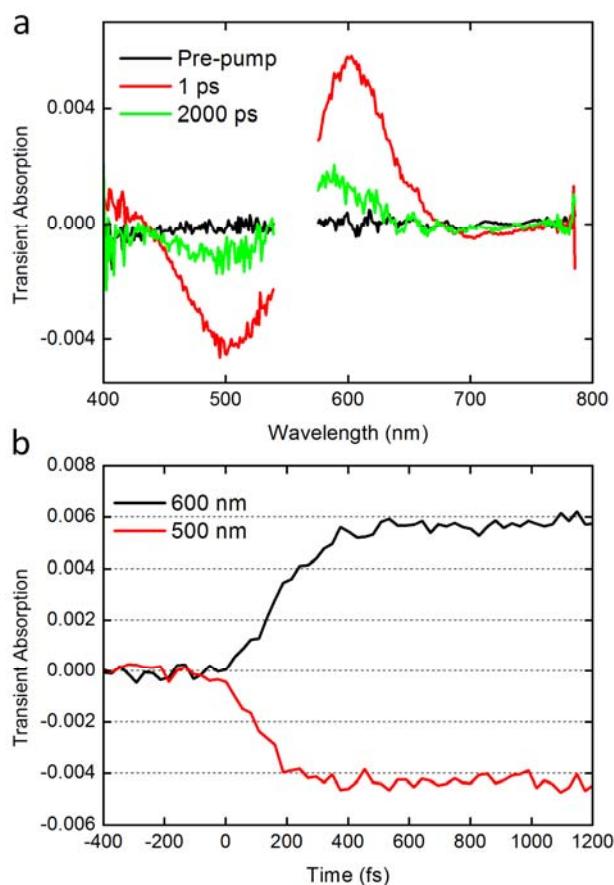
These results confirm that a significant proportion of excited molecules of **1** and **2** relax to the ground state from a singlet excited state with a much larger dipole moment. The poor solubility of **1** and **2** in most solvents prevents us performing a Lippert-Mataga analysis to extract the change in dipole moment in the excited state relative to the ground state, however this has been performed for a very similar perylene monoimide substituted at the *peri*-position by benzoic acid, showing an increase in dipole moment of 16 Debye upon photoexcitation⁸. As discussed in the main text, intramolecular charge transfer from the core-substituted phenylene-ethynylene to the photoexcited perylene monoimide is the likely cause.



Supplementary Figure S4| Absorption and emission of 1 and 2 in ethanol. Normalised absorption spectra of **1** (green curve) and **2** (black curve) and normalised emission spectra of **1** (blue curve) and **2** (red curve).

Confirmation of photoinduced intramolecular charge transfer in **2** comes from transient absorption spectroscopy, following 150 fs pulse width excitation of the perylene monoimide

subunit at 555 nm in aerated methanol (Fig. S5). Ground state depletion at 500 nm occurs within the pulse width, however the transient absorption at 600 nm grows in over ~ 0.6 ps and is attributed to the intramolecular charge transfer state (the perylene monoimide anion radical absorbs at 600 nm⁹, and the cation radical of phenylacetylene at 620 nm¹⁰). The grow-in is characteristic of intramolecular vibrational relaxation and solvation of excited states that are very different in conformation or electronic distribution from their geminate ground state. After 2 ns, the majority of the transient absorption has decayed, in keeping with the fluorescence lifetime of 4 ns, suggesting that the intramolecular charge transfer state decays to the ground state.

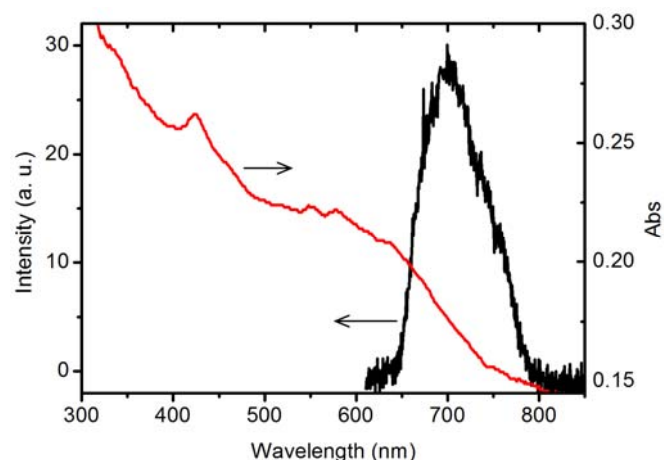


Supplementary Figure S5| Transient absorption spectroscopy of 2 in aerated methanol. **a**, Transient absorption spectra before (black curve), and then 1 ps (red curve) and 2 ns (green curve) after 150 fs pulse-width excitation of the perylene monoimide (excitation wavelength 555 nm, this region removed from spectra due to excessive light scattering). **b**, Kinetics of formation of the ground state depletion signal at 500 nm (red curve)

and of the transient absorption at 600 nm (black curve), attributed to photoinduced intramolecular charge transfer.

Unsubstituted perylene monoimide has a fluorescence quantum yield of 0.99 and a fluorescence lifetime of 5.0 ns in toluene and benzonitrile¹¹. The comparative quenching of perylene monoimide fluorescence in **1** and **2** shows that there are also significant non-radiative relaxation pathways operating, enhanced for **1** over **2** perhaps due to the direct connection of the perylene monoimide chromophore to the ethynylene unit in **1** and hence stronger electronic coupling. Vibrational relaxation to the ground state (internal conversion) or intersystem crossing to form either a non-intramolecular charge transfer triplet state or an intramolecular charge transfer triplet state¹⁰ are all possible 'dark' relaxation pathways.

While deposition of single molecules of **3** on glass, spin-cast from $\sim 10^{-9}$ M ethanol solutions, is clearly evident from the defocused wide-field fluorescence imaging (Video S3), at the $\sim \mu\text{M}$ concentrations required for bulk solution photophysical studies, aggregation occurs. This is evident in the broadening of the absorption spectrum of **3** (Fig. S6). A clear fluorescence maximum is evident at 700 nm. An accurate fluorescence quantum yield could not be determined, and multi-exponential fluorescence decay kinetics were observed.



Supplementary Figure S6| Absorption and emission spectra of **3 in ethanol.** The absorption spectrum (red curve) and emission spectrum (black curve) of **3** in aerated ethanol.

Given a fluorescence lifetime of 4 ns, an absorption coefficient of $\sim 50,000 \text{ M}^{-1}\text{cm}^{-1}$ at 532 nm, and an excitation power density $\sim 2 \text{ kW/cm}^2$, single molecule excitation rates of **2** are expected to be in the range 10^6 sec^{-1} . A similar estimation can be made for **3** from literature values.

Section S8: Description of Supplementary Videos.

Video 1, Consecutive defocused wide-field fluorescence microscopy images of single molecules of **2** on glass under a PnBMA over-layer at $T = 293$ K (532 nm quasi-TIRF excitation, the direction of propagation of the evanescent field is close to the left/right axis of the video). Most molecules remain locked in fixed orientations for the duration of the video due to the rigidity of the PnBMA overlayer ($T_g = 296$ K). The video runs in real time (500 ms image integration time, 2 frames per second, 268 frames in total, 134 seconds duration for the experiment). Image dimensions are 320 x 240 pixels, corresponding to 15.5 x 11.6 μm on the sample.

Video 2, Consecutive defocused wide-field fluorescence microscopy images of single molecules of **2** on glass under a PnBMA over-layer at $T = 315$ K (532 nm quasi-TIRF excitation, the direction of propagation of the evanescent field is close to the left/right axis of the video). The orientations of the molecules are predominantly in-plane (polar angles 60–90°) and show rapid re-orientation for the duration of the video due to the increased free volume in the PnBMA matrix at $T = 315$ K ($T_g = 296$ K). The video runs 8 times slower than real time (30 ms integration time, 600 frames, 18.3 seconds duration for the experiment. The video runs at 4 frames per second for 150 seconds). Image dimensions are 320 x 240 pixels, corresponding to 15.5 x 11.6 μm on the sample.

Video 3, Consecutive defocused wide-field fluorescence microscopy images of single molecules of **3** on glass under a PS over-layer at $T = 308$ K. For the first 40 seconds of the video, 640 nm circularly polarized excitation was employed, aligned along the optical axis of the microscope. The orientations of the molecules are predominantly in-plane (polar angles 60°–90°) with no obvious tendency for any in-plane direction, as expected for an azimuthal Brownian rotor. For the last 40 seconds of the video, excitation was adjusted to approach the sample at a high angle (quasi-TIRF excitation), resulting in dramatically improved signal-to-noise ratio. The direction of propagation of the evanescent excitation field is close to the top/bottom axis of the video. The molecules continue to rotate but clearly spend more time oriented along the left/right axis of the video (perpendicular to the direction of evanescent field propagation, *i.e.* aligned with the maximum in-plane evanescent field amplitude). These molecules orientations over time are included in the frequency histograms in Fig. 3f and g of the main article. The video runs 10 times faster than real time (1 sec integration time, 800 frames, 13.33 minutes experiment duration. The video runs at 10 frames per second for 80 seconds). Due to the long duration of the experiment, it was necessary to correct for focal plane drift (for instance at 33 seconds, and at 1 minute, 14 seconds in the video). Image dimensions are 320 x 240 pixels, corresponding to 15.6 x 11.7 μm on the sample.

Section S9: References

1. Böhmer, M. & Enderlein J. Orientation imaging of single molecules by wide-field epifluorescence microscopy. *J. Opt. Soc. Am. B* **20**, 554–559 (2003).

2. Patra, D., Gregor, I. & Enderlein, J. Image analysis of defocused single-molecule images for three-dimensional molecule orientation studies. *J. Phys. Chem. A* **108**, 6836-6841 (2004).
3. Uji-i, H. *et al.* Defocused Imaging in Wide-Field Fluorescence Microscopy. *Fluorescence of Supramolecules, Polymers, and Nanosystems* (Springer, Berlin, 2008).
4. Deres, A. *et al.* The origin of heterogeneity of polymer dynamics near the glass temperature as probed by defocused imaging. *Macromol.* **44**, 9703 (2011).
5. Lu, C.-Y. & Vanden Bout, D. A. Effect of finite trajectory length on the correlation function analysis of single molecule data. *J. Chem. Phys.* **125**, 124701 (2006).
6. Mackowiak, S. A. & Kaufman, L. J. When the heterogeneous appears homogeneous: discrepant measures of heterogeneity in single-molecule observables. *J. Phys. Chem. Letts.* **2**, 438-442 (2011).
7. Wakelin, S. & Bagshaw, R. A prism combination for near isotropic fluorescence excitation by total internal reflection. *J. Microsc.* **209**, 143-148 (2003).
8. Margineanu, A. *et al.* Visualization of membrane rafts using a perylene monoimide derivative and fluorescence lifetime imaging. *Biophys. J.* **93**, 2877-2891 (2007).
9. Gosztola, D., Niemczyk, M. P., Svec, W., Lukas, A. S. & Wasielewski, M. R. Excited Doublet States of Electrochemically Generated Aromatic Imide and Diimide Radical Anions, *J. Phys. Chem. A* **104**, 6545-6551 (2000).
10. Flors, C. *et al.* Energy and electron transfer in ethynylene bridged perylene diimide multichromophores. *J. Phys. Chem. C* **111**, 4861-4870 (2007).